Am J Cancer Res 2023;13(7):3013-3026
www.ajcr.us /ISSN:2156-6976/ajcr0149627

Original Article

HSP105 suppresses the progression of cutaneous squamous cell carcinoma by activating the P53 signaling pathway

Meng Jia, Kai-Yi Zhou, Li-Jia Deng, Sheng Fang

Department of Dermatology, The First Affiliated Hospital of Chongqing Medical University, Chongqing, China

Received February 12, 2023; Accepted June 20, 2023; Epub July 15, 2023; Published July 30, 2023

Abstract: Cutaneous squamous cell carcinoma (cSCC) is a common type of nonmelanoma skin cancer with a very high incidence. Heat shock proteins (HSPs) are involved in abnormal proliferation, invasion and apoptosis of tumor cells. Whether HSP105 acts as a promoter or inhibitor of cSCC remains to be further explored. This study investigated the biological role of HSP105 in the progression of cSCC. Real-time PCR and Western blotting were used to detect the mRNA and protein expression of HSP105 in cSCC cell lines. Cell lines with overexpression and knockdown of HSP105 were established to analyze their cell cycle distribution, proliferation, apoptosis, migration, invasion and biological mechanisms. Finally, the proliferative effect of HSP105 in cSCC cells was verified in nude mice. We found that HSP105 expression was decreased in cSCC cell lines. Overexpression of HSP105 in A431 and SCL-1 cell lines induced cell cycle arrest and apoptosis, inhibited cell proliferation, reduced cell migration and invasion, and inhibited tumor growth in vivo. The opposite result was observed in the HSP105-silenced cell lines. Furthermore, HSP105 activated the P53 signaling pathway and exerted anticancer effects. Our findings provide new perspectives on the critical role and potential mechanisms of HSP105 in the development of cSCC, suggesting that HSP105 may be a novel therapeutic target for cSCC.

Keywords: HSP105, cutaneous, squamous cell carcinoma, P53, suppresses

Introduction

Cutaneous squamous cell carcinoma (cSCC) is the most common form of metastatic skin cancer, accounting for at least 20% of all skin cancer-related mortality with an increasing prevalence and incidence worldwide. The prognosis of advanced or metastatic cSCC is poor due to the absence of defined biomarkers to assess the risk of metastasis or specific therapeutic targets [1]. It is essential to elucidate the molecular mechanisms of cSCC to discover novel immunotherapeutic targets for cSCC.

Heat shock proteins (HSPs), synonymous with molecular chaperones, are involved in aberrant proliferation, invasion and apoptosis of tumor cells [2]. HSP105 belongs to the HSP110 family, which plays a central role in protein stabilization and signaling pathways and has emerged as a new target for cancer chemotherapy [3]. Functionally, HSP105 contributes to protein function by maintaining denatured protein substrates in a soluble, foldable state to facilitate ligand binding [4]. The high metabolic demand and unlimited proliferative capacity of tumor cells dramatically alter the nutrient composition of the tumor environment [5]. Therefore, tumor cells depend on the folding mechanism of HSP105 to maintain their homeostasis. However, other studies have demonstrated that HSP105 is capable of not only refolding misfolded proteins but also folding other denatured proteins into their original conformation [6]. Whether blocking the function of HSP105 will eliminate the development of cancer remains to be determined and deserves further study.

A group of researchers demonstrated that HSP105 is overexpressed in several human tumors, such as cervical cancer, bladder cancer, lung cancer, and squamous cell carcinoma of the tongue [7]. Elevated expression of HSP105 is a factor of poor prognosis in patients

with melanoma, non-Hodgkin lymphoma esophageal cancer, gastric cancer, colorectal cancer, MDS or AML [8, 9]. Yu N and coworkers observed that HSP105 overexpression predicts a decline in the survival of breast cancer patients [10]. However, prolonged survival of bladder cancer patients was found to be dependent on higher HSP105 expression in other studies [11]. A study by Zheng Y et al. demonstrated that HSP105 inhibits the growth of renal cell carcinoma in mice [12]. Increased expression of HSP105 in colorectal cancer cells induced the production of macrophages, which have a strong anti-inflammatory effect and thus inhibit the development of colorectal cancer [13]. Our previous study found that HSP105 was highly expressed in the normal epidermis and showed a decreasing trend in cSCC, suggesting that it has an anticancer effect [14]. Therefore, whether HSP105 acts as a promoter or inhibitor of cSCC remains to be further explored. This study investigated the biological role of HSP105 in cSCC progression while exploring the potential mechanism.

Materials and methods

Cell culture and lentivirus transfection

Human epidermoid carcinoma (A431), SCL-1 and human keratinocyte (HaCaT) cell lines were purchased from Chongqing Biospes Co., Ltd. All cell lines were maintained in DMEM containing 10% fetal bovine serum (Gibco, Carlsbad, USA) and 1% penicillin and streptomycin (Gibco, Carlsbad, USA). Cells were routinely cultured in a humidified incubator containing 5% CO_2 at 37°C. Lentiviral particles encoding shRNA against HSP105 (sh-HSP105), control sequence (sh-con) and an HSP105 overexpression sequence (LV-HSP105), and control gene (LV-con) were prepared by Shanghai Genechem Co., Ltd. Cells were seeded on 24-well plates (5×10^4/well), cultured for 24 h and then transfected with lentivirus for 10 h. Finally, the transfection efficiency was measured after 2~3 days of screening with puromycin.

Real-time PCR

Total cellular RNA was extracted from A431 and SCL-1 cells using the Steady Pure Universal RNA Extraction Kit (Accurate Biology, AG21017, China) according to the manufacturer's instructions. cDNA synthesis was performed using an Evo M-MLV Mix Kit with gDNA Clean for qPCR (Accurate Biology, AG11728, China). Finally, real-time quantitative PCR was performed using a SYBR Green Premix Pro Taq HS qPCR Kit (Accurate Biology, AG11701, China) and detected on a CFX96™ real-time PCR detection system (Bio-Rad Laboratories, USA). GAPDH was used as an internal control to normalize expression. The $2^{-\Delta\Delta Ct}$ method was used to analyze the relative expression levels.

Western blot

The primary antibodies used in the Western blot analysis included HSP105 (1:5,000), p21 (1:1,000), Cyclin D1 (1:1,000), MMP9 (1:1,000), MMP2 (1:1,000), P53 (1:1,000), MDM2 (1:1,000), CDK4 (1:1,000), Bcl-2 (1:1,000), Bax (1:1,000) and GAPDH (1:5,000). The secondary antibodies used were HRP-c conjugated Affinipure Goat Anti-Mouse IgG (H+L) (1:5,000) and Goat Anti-Rabbit IgG (H+L) (1:5,000). All antibodies were purchased from Proteintech, except for HSP105, which was obtained from Abcam in the United States.

Cells cultured in six-well plates were placed on ice, washed three times with prechilled PBS, and then lysed by adding RIPA buffer to obtain total cellular protein. Different protein samples were aspirated and added to each well of the 8% or 10% SDS-PAGE gel for electrophoresis. After electrophoresis was completed, proteins on SDS-PAGE gels were transferred to 0.45 μm PVDF membranes (Millipore, USA). The membranes were blocked at room temperature with QuickBlock™ Blocking Buffer for Western blot (Beyotime, Shanghai, China) for 15 min and then incubated overnight at 4°C with the corresponding primary antibody. The following day, the incubated membranes were washed three times with TBST and subsequently incubated with the secondary antibody for 1 h at room temperature. Finally, the membranes were rinsed again with TBST, and the signal was detected with an Odyssey fluorescence scanner. Grayscale values of protein bands were analyzed using ImageJ software (NIH Image, Bethesda, MD), with GAPDH as an internal reference.

Cell proliferation assay

The cell proliferative capacity of A431 and SCL-1 cells was determined by Cell Counting

Kit-8 (CCK-8) (MedChemExpress, USA). Cells were seeded in 96-well plates at a density of 2000 cells/well, and 5 replicate wells were used for each cell line to reduce errors, while 100 μl of PBS was added to the edge circles to avoid evaporation. Ten microliters of CCK-8 reagent were added to each well at 0, 24, 48, 72 and 96 hours after plating. The plate was incubated for 3 h. When the color changed to orange, the 96-well plate was placed in a microtiter plate reader, and the absorbance was detected at a wavelength set to 450 nm.

Cell cycle analysis

Cells were seeded in six-well plates, harvested when fully grown, fixed with 100 μL of PBS and 900 μL of prechilled 75% ethanol, and mixed by gentle blowing. The fixed cells were rewashed with prechilled PBS, the supernatant was discarded, 100 μL of RNase A (Sigma-Aldrich, St. Louis, USA) was added to entirely suspend the cells, and the cells were incubated in a water bath at 37°C for 30 min, followed by the addition of PI solution at 4°C. Finally, flow cytometry was used to measure cellular DNA content, and cell cycle analysis was conducted using ModFit LT software (Verity Software House, Topsham, ME).

Cell apoptosis assay

After the cells in the 6-well plate were fully grown, the floating cells were first placed in a centrifuge tube, and then, the cells were collected with 0.25% trypsin (without EDTA) and washed with PBS. Finally, 1×10^6 cells were resuspended in 500 μl of PBS (pH = 7.2) buffer in a 1.5 ml EP tube for apoptosis detection. The collected groups of cells were washed twice with precooled PBS, and cell suspensions (1×10^6 cells/well) were made by adding 1× Annexin V binding buffer. One hundred microliters of cell suspension were placed in a culture tube and centrifuged, and the supernatant was discarded. Annexin V-FITC conjugate was added to resuspend the cells, which were incubated for 10 min at room temperature and protected from light. Cells were resuspended by adding 190 μl of Annexin V-FITC conjugate and 10 μl of propidium iodide staining solution. The percentage of apoptosis was measured immediately by flow cytometry. Each experiment was repeated three times.

Wound-healing assay

Cell migration was assessed using a wound-healing assay. Groups of cells were seeded in six-well plates, and when the cells reached 90% confluence, a scratch was made in each well with the tip of a 200-μL pipette. Cells were rinsed with PBS, and 3 ml of DMEM without FBS was added to each well for incubation. The slit area of each cell sample was evaluated at 0, 24 and 48 h and measured by ImageJ software. Cell migration was indicated as a percentage of (initial slit width - 48 h slit width)/initial slit width, with slit width = area/length.

Cell invasion assay

Microporous filter membranes inside Transwell chambers were infiltrated with 50 μL of matrix gel (Corning, USA) per well before the experiment, and the chambers were placed on 24-well plates and incubated overnight in a cell culture incubator to allow sufficient fusion. Cells were resuspended in 200 μL of DMEM without FBS and inoculated into the upper cell compartment (1×10^5 cells/well), and 700 μL of DMEM with 10% FBS was added to the lower cell compartment. The chambers were routinely incubated in an incubator for 36 h. The cell chamber was removed, and the Matrigel and upper chamber were gently wiped with a moistened cotton swab. A new 24-well plate was taken, and 600 μL of 4% paraformaldehyde was added. The fixative was discarded, stained with 0.1% crystalline violet for 10 min, and washed with PBS. After proper air drying, five fields of view were randomly selected under a light microscope at 200× magnification to observe the cells and count them.

Coimmunoprecipitation

Forty microliters of protein A/G magnetic beads (MCE, HY-K0202) was added to PBST and washed twice, and the beads were magnetically separated. Then, 400 μl of PBST and 2 μg HSP105 antibody (Abcam), 2 μg P53 antibody (Proteintech) and 2 μg rabbit IgG antibody (Beyotime) were added, and the cells were fully reacted at 4°C. The cells were lysed by adding 14 μl of protease inhibitor cocktail (MCE) to 1400 μl of IP lysate (Beyotime), left on ice for 30 min, and centrifuged at 16000 × g for 15 min at 4°C, and the supernatant was removed and set aside. For magnetic separation of mag-

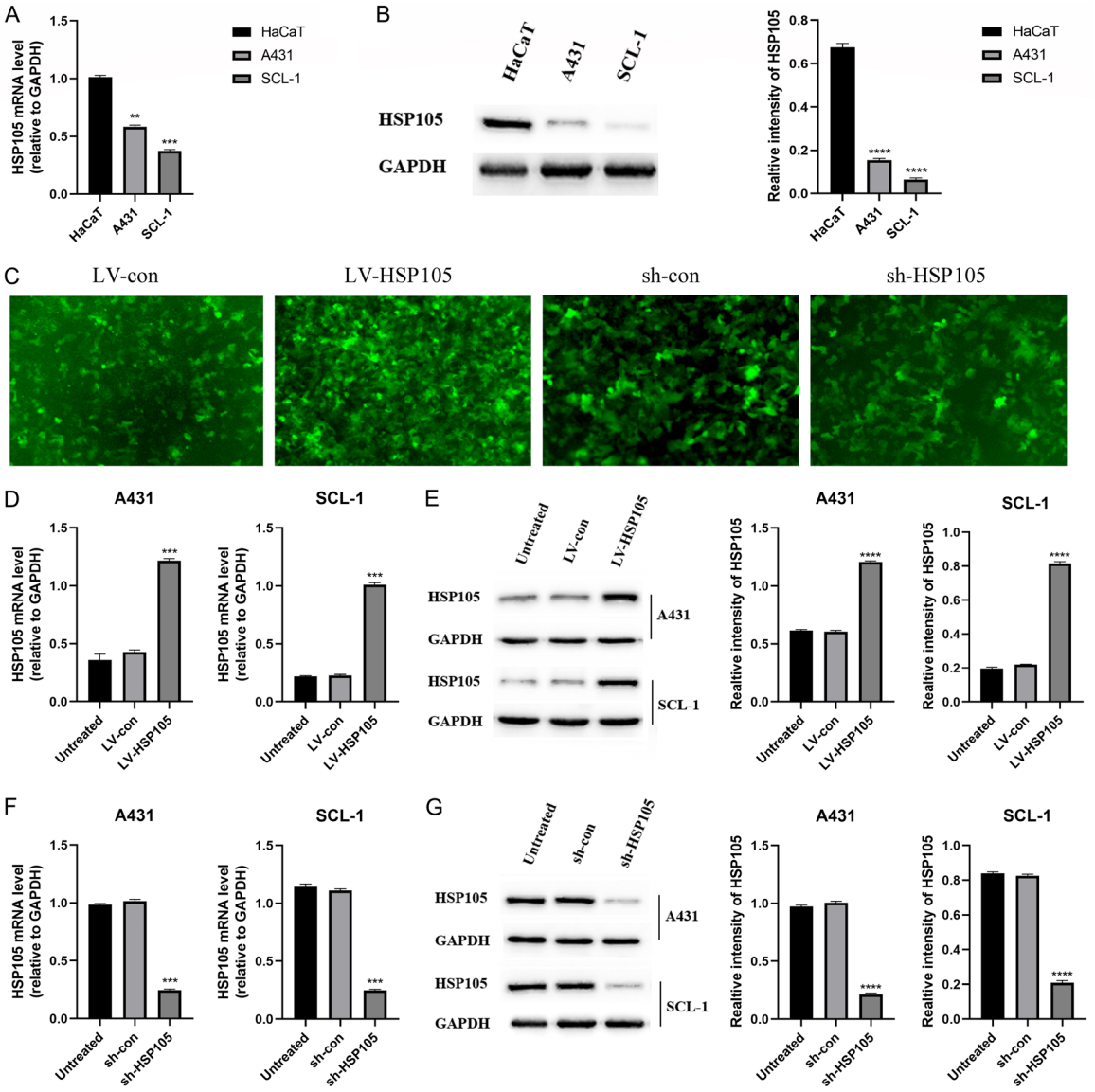

Figure 1. Downregulation of HSP105 expression in cSCC cells. (A) Real-time PCR and (B) Western blot analysis of HSP105 expression in HaCaT human keratinocytes and two cSCC cell lines (A431 and SCL-1). GAPDH was used as a loading control. (C) HSP105 overexpression and knockdown vectors and their negative controls were transfected with lentiviral efficiency up to 90%. HSP105 was stably overexpressed in LV-HSP105 cells compared to untreated and LV-con cells by (D) real-time PCR and (E) Western blot analysis. Stable knockdown of HSP105 expression in sh-HSP105 cells compared to untreated and sh-con cells by (F) real-time PCR and (G) Western blotting analysis. All results are presented as the mean ± SEM using one-way ANOVA in at least three independent experiments. **P < 0.01, ***P < 0.001, ****P < 0.0001, compared to the untreated group.

netic beads, 400 μl of the above supernatant was added to 3 EP tubes with different antibodies and rotated overnight at 4°C. After the reaction was completed, the beads were magnetically separated and transferred to new EP tubes, 30 μl of 1× loading buffer was added to each EP tube after aspirating the buffer, and 25 μl of 5× loading buffer was added to the aforementioned 100 μl of supernatant in a metal bath for 10 min at 95°C to prepare the upper sample for SDS-PAGE and subsequent protein detection.

In vivo tumor growth assay

Female nude mice (four to five weeks old) were purchased from GemPharmatech (Jiangsu, China). The mice were randomly divided into five groups (n = 5/group, untreated, LV-con, LV-HSP105, sh-con, sh-HSP105). All mice were

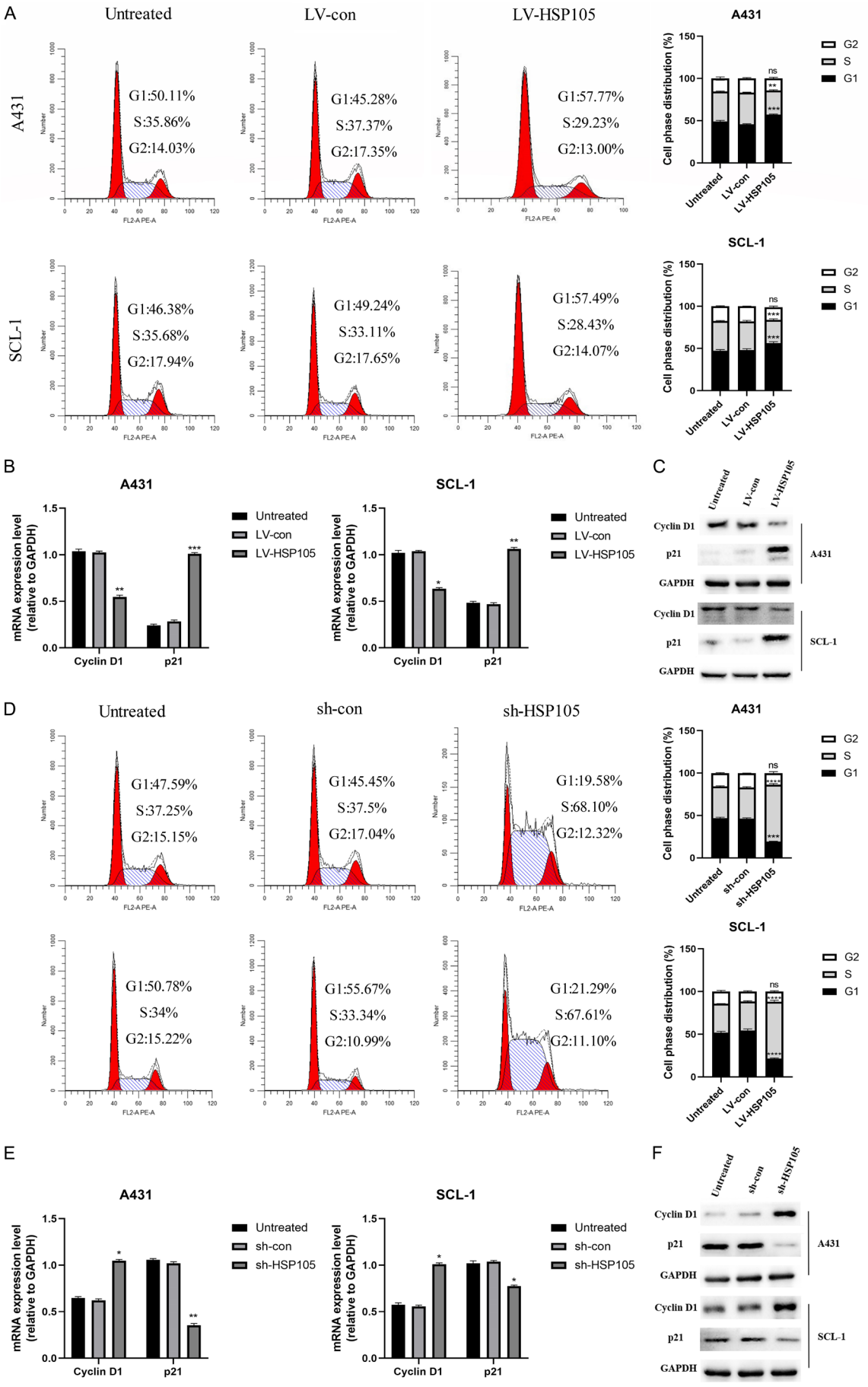
A
Untreated
LV-con
LV-HSP105
A431
SCL-1
G1:50.11%
S:35.86%
G2:14.03%
G1:45.28%
S:37.37%
G2:17.35%
G1:57.77%
S:29.23%
G2:13.00%
G1:46.38%
S:35.68%
G2:17.94%
G1:49.24%
S:33.11%
G2:17.65%
G1:57.49%
S:28.43%
G2:14.07%
Number
FL2-A PE-A
Cell phase distribution (%)
G2
S
G1
ns
B
mRNA expression level (relative to GAPDH)
Cyclin D1
p21
C
GAPDH
D
sh-con
sh-HSP105
G1:47.59%
S:37.25%
G2:15.15%
G1:45.45%
S:37.5%
G2:17.04%
G1:19.58%
S:68.10%
G2:12.32%
G1:50.78%
S:34%
G2:15.22%
G1:55.67%
S:33.34%
G2:10.99%
G1:21.29%
S:67.61%
G2:11.10%
E
F

Figure 2. HSP105 induces cell cycle arrest in G0/G1 phase through regulation of cell cycle-related genes. (A) Flow cytometric cycle assay showed that HSP105-overexpressing cells were arrested in G1 phase. The (B) real-time PCR and (C) Western blot analysis showed that overexpression of HSP105 inhibits cell proliferation by decreasing Cyclin D1 expression and increasing p21 expression. (D) Cell cycle profiles following HSP105 knockdown were analyzed by flow cytometry. (E) Real-time PCR and (F) Western blot analysis showed that HSP105 deficiency promotes cell proliferation by increasing Cyclin D1 expression and inhibiting p21 expression. All results are presented as the mean ± SEM using one-way ANOVA in at least three independent experiments. *P < 0.05, **P < 0.01, ***P < 0.001, ****P < 0.0001, compared to the untreated group.

acclimatized and fed in an animal room at 22°C and allowed to drink and eat ad libitum. SCL-1 cells (2×10^6 per animal) were injected subcutaneously into the right axilla of mice. Tumor growth was measured with digital calipers, and tumors were weighed weekly. Tumor volume was assessed by the following formula: volume (mm^3) = $width^2 \times length/2$. All mice were sacrificed 5 weeks after injection, and tumor tissue was dissected and weighed. All animal experiments were approved by the Institutional Animal Care and Use Committee of the First Hospital of Chongqing Medical University.

Statistical analysis

All data were statistically analyzed using GraphPad Prism 9.0.0 software (GraphPad Software, San Diego, California) and SPSS software for Windows (version 26.0; SPSS, Inc.). All data tested by the Shapiro-Wilk test were normally distributed, and statistical significance was calculated by one-way ANOVA. Each group of experiments was repeated at least three times, and a *P* value < 0.05 was considered statistically significant.

Results

Downregulation of HSP105 expression in cSCC cells and lentivirus transfection

Our previous study showed that HSP105 expression was downregulated in cSCC human tissues and closely correlated with clinicopathological characteristics [14]. Here, we validated this result in A431 and SCL-1 cell lines, which revealed decreased expression of HSP105 in cSCC cells compared to HaCaT cells (**Figure 1A**, **1B**).

Given that HSP105 expression was downregulated in cSCC, we hypothesized that HSP105 might suppress cSCC development. To test the potential anticancer effect of HSP105, we further overexpressed and knocked down HSP105 in A431 and SCL-1 cells with a lentiviral vector, and the immunofluorescence efficiency of lentiviral transfection was as high as 80-90% (**Figure 1C**), which was confirmed by real-time PCR and Western blot analysis (**Figure 1D-G**).

Overexpression of HSP105 causes cell cycle arrest in cSCC

The uncontrolled proliferation of cancer cells is known to result from disruption of the cell cycle and mutations in genes that regulate the cell cycle [14]. To investigate the effect of HSP105 on cell cycle progression, we assessed cell cycle distribution using flow cytometry. The cell cycle results showed that the overexpression of HSP105 resulted in an increased proportion of the G0/G1 phase, a decreased ratio of the S phase, and almost no change in the G2 phase, which led to growth arrest of A431 and SCL-1 cells at the G1/S phase transition (**Figure 2A**). As expected, overexpression of HSP105 decreased Cyclin D1 expression while upregulating p21 expression in A431 and SCL-1 cells (**Figure 2B**, **2C**).

We similarly analyzed the effect of HSP105 knockdown on cell development and showed that HSP105 knockdown promoted the growth of A431 and SCL-1 cells, accompanied by elevated Cyclin D1 and downregulation of p21 (**Figure 2D-F**).

Overexpression of HSP105 inhibits the proliferation of cSCC cells and induces apoptosis

We analyzed the proliferation of A431 and SCL-1 cells at 0, 24, 48, 72, and 96 hours by Cell Counting Kit-8 assays (CCK-8) and showed that significant inhibition of cSCC cell proliferation was achieved by overexpression of HSP105 (**Figure 3A**). To verify whether HSP105 regulates apoptosis in cSCC cells, we detected apoptosis by flow cytometry. Untreated or negative control lentivirus-transfected A431 and SCL-1 cells had a low basal apoptosis rate of 1-4%. However, overexpression of HSP105

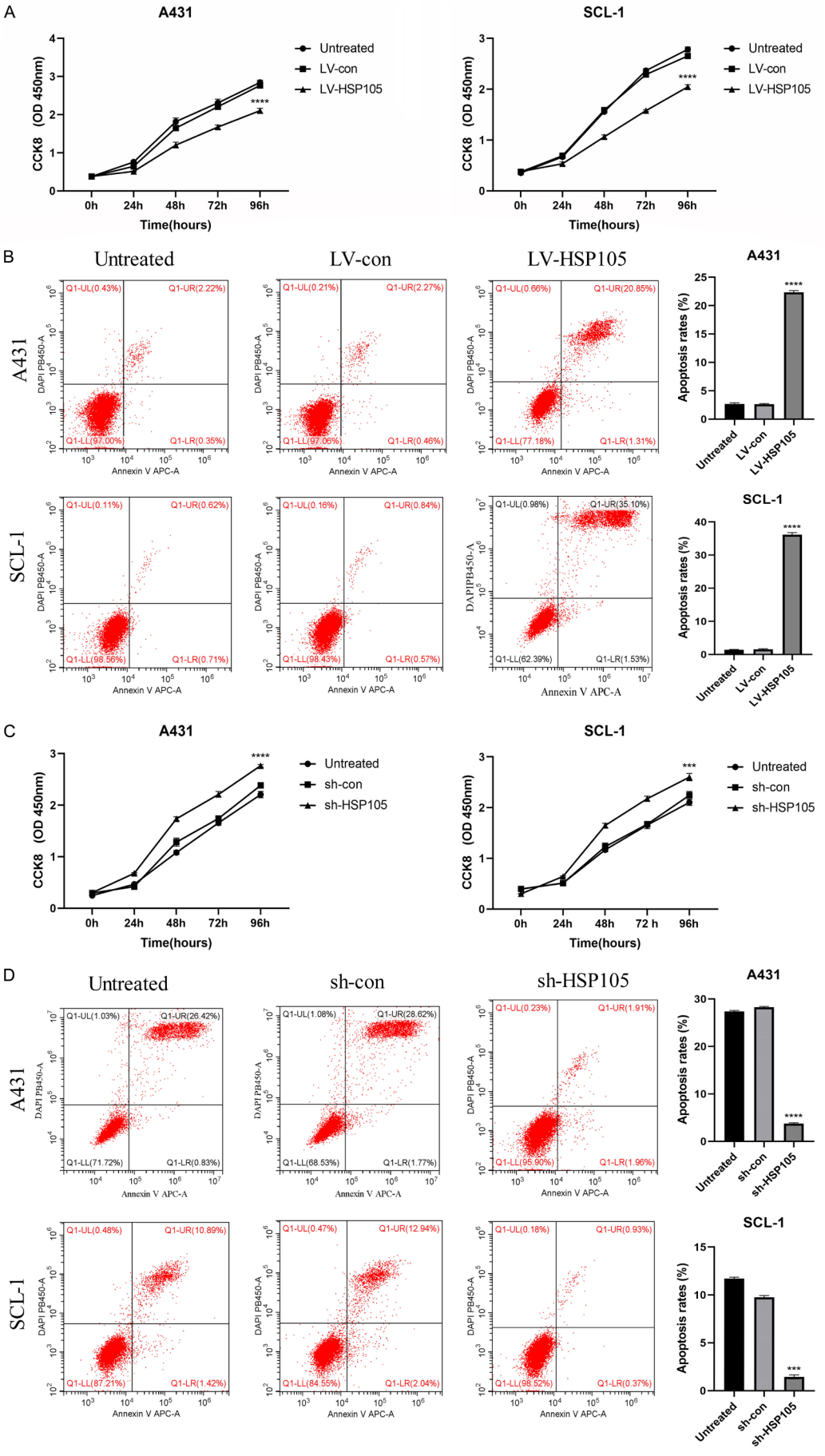
A
A431
SCL-1
CCK8 (OD 450nm)
Time(hours)
0h
24h
48h
72h
96h
Untreated
LV-con
LV-HSP105
****
B
Untreated
LV-con
LV-HSP105
A431
SCL-1
DAPI PB450-A
Annexin V APC-A
Q1-UL(0.43%)
Q1-UR(2.22%)
Q1-LL(97.00%)
Q1-LR(0.35%)
Q1-UL(0.21%)
Q1-UR(2.27%)
Q1-LL(97.05%)
Q1-LR(0.46%)
Q1-UL(0.66%)
Q1-UR(20.85%)
Q1-LL(77.18%)
Q1-LR(1.31%)
Q1-UL(0.11%)
Q1-UR(0.62%)
Q1-LL(98.56%)
Q1-LR(0.71%)
Q1-UL(0.16%)
Q1-UR(0.84%)
Q1-LL(98.43%)
Q1-LR(0.57%)
Q1-UL(0.98%)
Q1-UR(35.10%)
Q1-LL(62.39%)
Q1-LR(1.53%)
Apoptosis rates (%)
C
A431
SCL-1
sh-con
sh-HSP105
***
D
Untreated
sh-con
sh-HSP105
A431
SCL-1
Q1-UL(1.03%)
Q1-UR(26.42%)
Q1-LL(71.72%)
Q1-LR(0.83%)
Q1-UL(1.08%)
Q1-UR(28.62%)
Q1-LL(68.53%)
Q1-LR(1.77%)
Q1-UL(0.23%)
Q1-UR(1.91%)
Q1-LL(95.90%)
Q1-LR(1.96%)
Q1-UL(0.48%)
Q1-UR(10.89%)
Q1-LL(87.21%)
Q1-LR(1.42%)
Q1-UL(0.47%)
Q1-UR(12.94%)
Q1-LL(84.55%)
Q1-LR(2.04%)
Q1-UL(0.18%)
Q1-UR(0.93%)
Q1-LL(98.52%)
Q1-LR(0.37%)

Figure 3. HSP105 arrested proliferation and increased apoptosis in cSCC cells. A. CCK-8 assays detected the proliferation of HSP105 after overexpression treatment. B. Apoptosis of A431 and SCL-1 cells was measured by flow cytometry, and the rate of apoptosis was significantly increased after transfection with LV-HSP105. C. A431 and SCL-1 cell proliferation after HSP105 silencing was determined by the CCK-8 assay. D. After treatment of A431 and SCL-1 cells with 5-Fu for 24 h, the apoptosis rate was detected by flow cytometry, and 5-Fu-induced apoptosis could be inhibited upon HSP105 silencing. All results are presented as the mean ± SEM using one-way ANOVA in at least three independent experiments. ***P < 0.001, ****P < 0.0001, compared to the untreated group.

increased the apoptosis rate to 22-36% (**Figure 3B**). Moreover, we found that silencing HSP105 promoted the proliferation of cSCC cells (**Figure 3C**). The results showed that HSP105 knockdown protected A431 and SCL-1 cells from 5-Fu-induced apoptosis (**Figure 3D**).

Overexpression of HSP105 inhibits the migration/invasive ability of cSCC cells

Migration and invasion of tumor cells are important factors of tumor metastasis and are closely related to prognosis [15]. To ascertain the effects of HSP105 on cSCC cell migration and invasion, we performed wound healing and transwell assays, respectively. The results of the wound healing assay demonstrated that A431 and SCL-1 cells from LV-HSP105 had a smaller migratory area compared to the untreated and the negative control lentivirus groups (**Figure 4A**). Consistent with the results of the migration assay, the LV-HSP105 group showed a dramatic decrease in the total number of invading cells on the PET membrane compared to the other two control groups (**Figure 4B**).

Matrix metalloproteinase-2 (MMP-2) and matrix metalloproteinase-9 (MMP-9) are strongly associated with tumor infiltration and metastasis [16]. We further investigated the effect of HSP105 on the expression of MMP-2 and MMP-9 by real-time PCR and Western blotting. As shown in **Figure 4C**, **4D**, the expression of both MMP2 and MMP9 was decreased in the HSP105-overexpressing cells. We also found that the cells migrated over a larger area and were more invasive after HSP105 deficiency compared to the other two controls (**Figure 4E**, **4F**) with higher expression of MMP2 and MMP9 (**Figure 4G**, **4H**).

HSP105 inhibits cSCC cell growth by activating the P53 signaling pathway

In this study, we found that upregulation of HSP105 increased the protein expression of P53 and downregulated the cell cycle protein-dependent kinase CDK4. In addition, the elevation of HSP105 was accompanied by the upregulation of the proapoptotic protein Bax and cell cycle regulatory protein p21 and the downregulation of Bcl2 and CDK4 (**Figure 5A**, **5B**). In contrast, the reduction in HSP105 led to decreased P53 protein levels, downregulation of p21 and Bax, and upregulation of CDK4 and Bcl-2, which promoted cSCC cell proliferation and inhibited cSCC apoptosis (**Figure 5C**, **5D**). Second, MDM2, a central negative regulator of P53, showed an opposite trend to P53. Furthermore, co-IP results showed that there was an interaction between HSP105 and P53 (**Figure 5E**).

Overexpression of HSP105 inhibits tumor growth in a mouse model

To further confirm the effect of HSP105 on cSCC progression, we established xenograft tumor models in vivo with SCL-1 cell lines and measured body weight and tumor volume at the indicated time points. The results showed that there was no significant difference in body weight among the groups (**Figure 6A**). Importantly, overexpression of HSP105 delayed tumor cell growth, and silencing of HSP015 promoted tumor growth (**Figure 6B**). Five weeks after cell inoculation, tumor volume and weight were lower in the LV-HSP105 group than in the control group (**Figure 6C**), with the opposite result for sh-HSP105 (**Figure 6D**). These findings further suggest that HSP105 overexpression also has significant antitumor potential against cSCC in vivo.

Discussion

HSP105 has been considered a “danger signal” and is overexpressed in a variety of human cancers but is not expressed in normal tissues except the testis [17]. However, HSP105 is overexpressed in both normal epidermis and dermis as a way to protect the skin from damage caused by UVB or its stressors in the skin [18]. Our previous study found a significant reduction in HSP105 expression in cSCC compared to the normal epidermis, which did not occur for HSP70 and HSP90 [14]. Several

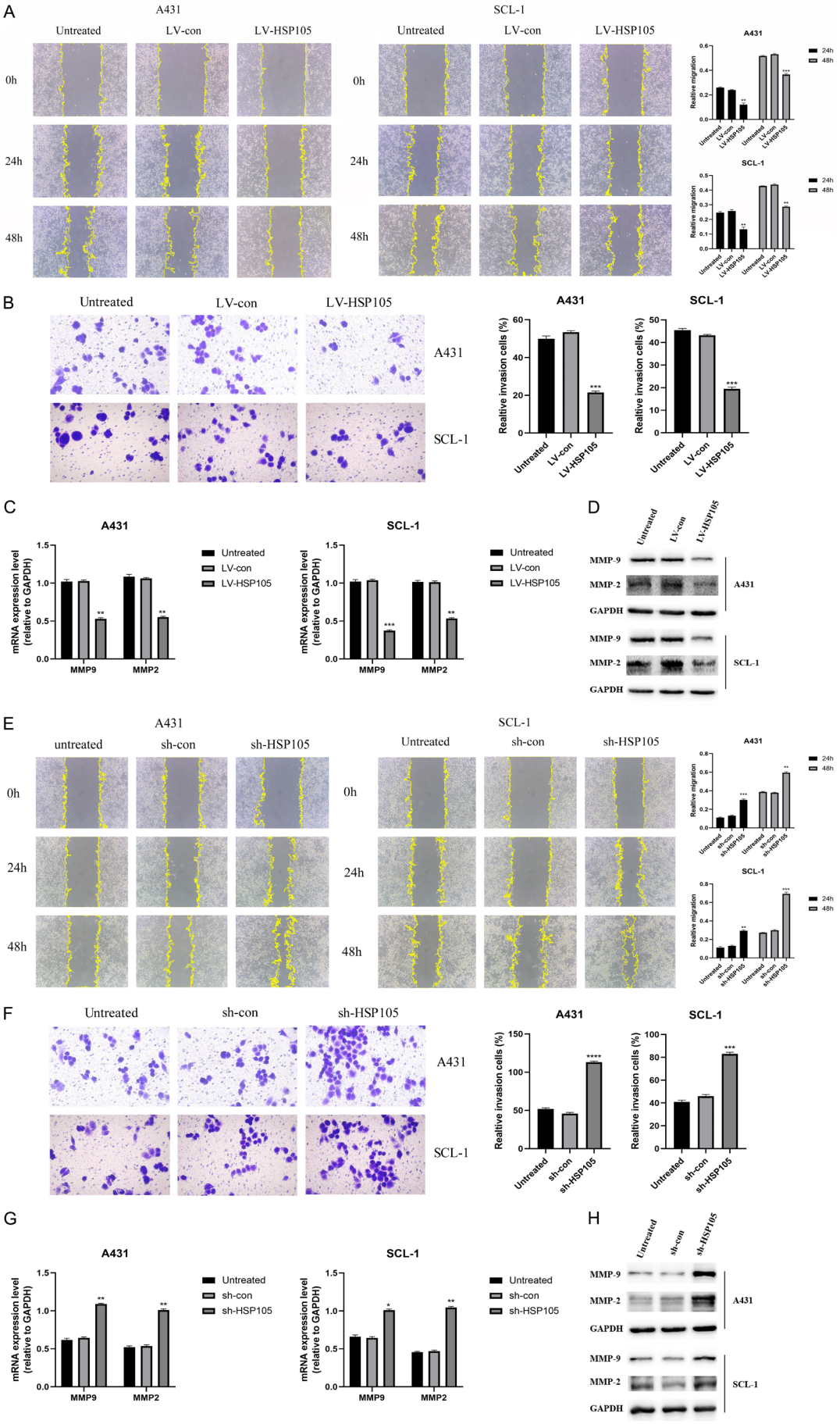
A
A431
SCL-1
Untreated
LV-con
LV-HSP105
0h
24h
48h
Realtive migration
24h
48h
B
A431
SCL-1
Realtive invasion cells (%)
C
mRNA expression level (relative to GAPDH)
MMP9
MMP2
D
MMP-9
MMP-2
GAPDH
E
untreated
sh-con
sh-HSP105
F
G
H

Figure 4. HSP105 suppresses cSCC cell migration and invasion. (A) LV-HSP105 transfection resulted in a smaller migration area in A431 and SCL-1 cells. (B) Transwell assays showed that cell invasion was reduced after HSP105 overexpression. The results of (C) real-time PCR and (D) Western blot analysis showed reduced expression levels of MMP-2 and MMP-9 in the HSP105-overexpressing A431 and SCL-1 cells. (E) sh-HSP105 transfection resulted in a larger migration area in A431 and SCL-1 cells. (F) Enhanced cell invasion after HSP105 silencing. (G) Real-time PCR and (H) Western blot analysis showed elevated expression levels of MMP-2 and MMP-9 in A431 and SCL-1 cells with HSP105 knockdown. All results are presented as the mean ± SEM using one-way ANOVA in at least three independent experiments. *P < 0.05, **P < 0.01, ***P < 0.001, ****P < 0.0001, compared to the untreated group.

reports have described the anti-inflammatory effects of extracellular HSP105, which can promote or inhibit inflammation [16, 19]. These findings suggest that the expression pattern of HSP105 varies with different sites and cell types. Since the role and molecular mechanisms of HSP105 in cSCC development have not been investigated, in the present study, we found that HSP105 expression was decreased in cSCC and that overexpression of HSP105 could inhibit cSCC cell proliferation, migration and invasion by activating P53 signaling while inducing apoptosis, thereby suppressing cSCC progression. Furthermore, overexpression of HSP105 significantly inhibited tumor growth in vivo.

The unlimited proliferation of cancer cells is preceded by a disruption of the cell cycle. Our study shows that HSP105 overexpression inhibits cSCC cell growth by reducing cyclin D1 and increasing the expression of p21. In contrast, knockdown of HSP105 reversed this pattern. The same regulatory effect of HSP105 on the cell cycle has been found in other studies. Our results are consistent with those of Kalos M et al., who found that HSP105 enhances cytotoxic T lymphocytes in cervical cancer, regulates cell proliferation and exerts antitumor effects [20]. Teshima H et al. used cell synchronization experiments to show that HSP105 silencing effectively promotes the mitotic transition from metaphase to anaphase by attenuating spindle assembly checkpoint (SAC) function [21].

HSP105 can inhibit cells from stress-induced apoptosis through the STAT3 and P53 signaling pathways [22]. Yamagishi N et al. showed that HSP105 inhibits apoptosis in HeLa cells by inhibiting the p38 MAPK signaling pathway [23]. However, our study showed that HSP105 overexpression promoted apoptosis in cSCC cells. This result might be because the expression pattern of HSPs varies depending on the stressor and cell type, and each heat shock protein has an essential and specific function in different tissues [24]. Scholars have investigated whether HSP105α inhibits apoptosis in neuronal PC12 cells while having a proapoptotic effect on embryonic F9 cells and showed that HSP105 has opposite effects on apoptosis, depending on the cell type [25, 26]. HSP105 truncation could protect colon cancer cells from TRAIL-induced apoptosis, while overexpression of HSP105 could block its antiapoptotic function, which is in line with our findings [27].

Abnormal migration and invasion of tumor cells are determinants of disease progression [28]. MMP was shown to be specifically expressed in cSCC cells and is an important regulator of cSCC cell invasion [29]. Our study showed that overexpression of HSP105 decreased the protein levels of MMP-2 and MMP-9, leading to impaired migration and invasion of cSCC cells. A previous study indicated that HSP70 deficiency contributes to aggravated brain injury by increasing the expression of MMP [30]. Ala-aho R et al. conducted a series of experiments on HSP105 and cSCC and found that P53 could effectively inhibit the expression of MMP in cSCC cells [31]. There is accumulating evidence that in mouse skin cancer models, P53 deficiency leads to more aggressive skin papilloma and promotes tumor growth [32].

cSCC has a wide range of mutant sites in the P53 gene, so an important early event in the development of cSCC is the mutation and inactivation of the tumor suppressor gene P53 [33]. HSP105 forms a complex with P53 at scrotal temperature and contributes to the stabilization of the P53 protein in the germ cell cytoplasm [34]. The P53 protein is located upstream of the cystatinase cascade, which is associated with HSPs, and some investigators found that the expression of the P53 protein was reduced after HSP105 siRNA treatment [35]. When cells are under stress, activated P53 promotes the transcription of the cell cycle regulator p21 and the proapoptotic gene Bax to induce cell cycle arrest and apoptosis [36]. Multiple lines of evi-

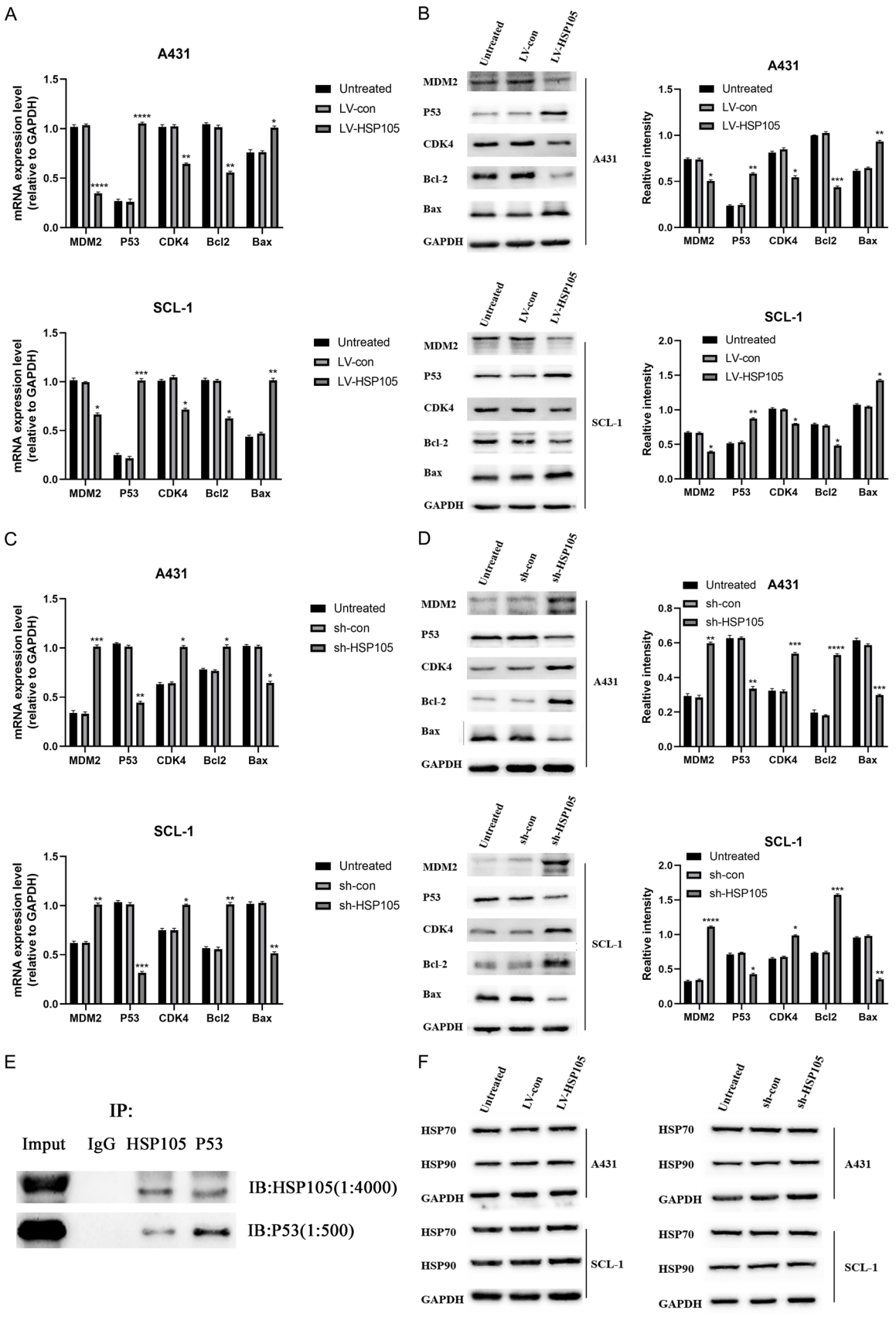

Figure 5. HSP105 suppresses cSCC cell growth by activating the MDM2/P53 signaling pathway. (A) Real-time PCR and (B) Western blot analysis showed that MDM2 protein levels were decreased and P53 protein levels were in-

creased in A431 and SCL-1 cells after HSP105 overexpression. Moreover, CDK4 was downregulated, while the apoptosis-related protein Bax was upregulated and Bcl2 was downregulated. (C) Real-time PCR and (D) Western blot analysis showed the opposite results when HSP105 was knocked down. Co-IP (E) results show that there is an interaction between HSP105 and P53. The expression of HSP90 and HSP70 did not change in response to the elevation or knockdown (F) of HSP105.

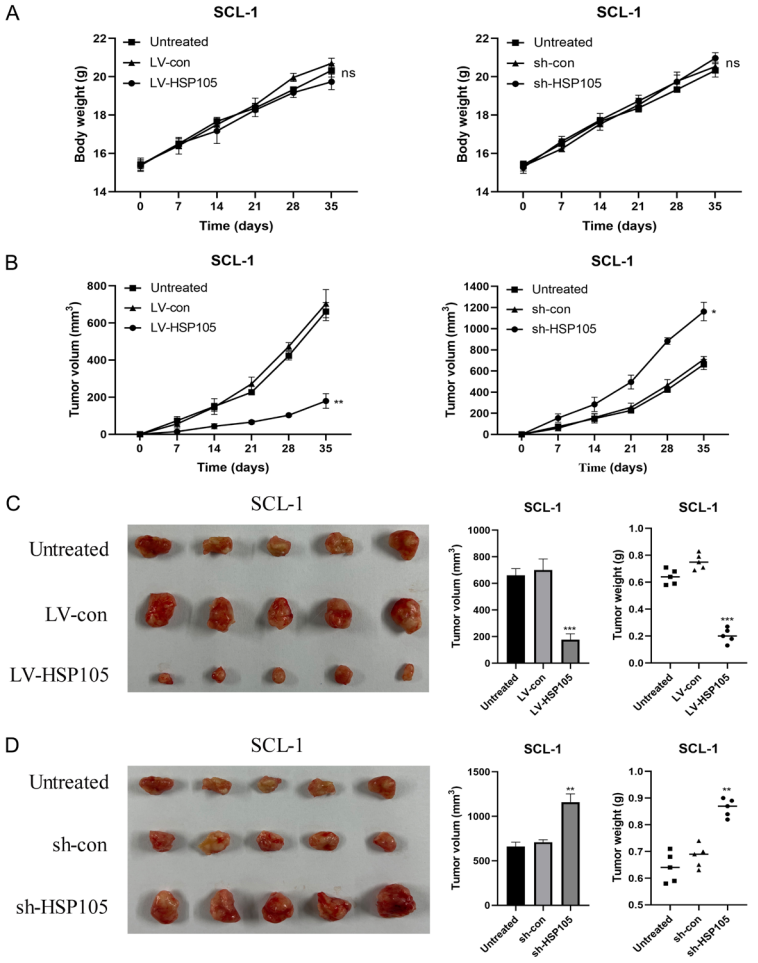

Figure 6. HSP105 overexpression inhibits tumor growth of cSCC in vivo. A. Body weight of NCG mice was measured and recorded weekly. B. Tumor volume was calculated via the width^2 × length/2 method at the indicated time point. C. HSP105 upregulation inhibits cSCC tumor growth. D. HSP105 downregulation promotes cSCC tumor growth. All results are presented as the mean ± SEM using Student's t test (n = 5). **P < 0.01, ***P < 0.001, compared to the untreated group.

dence suggest that under nonstress conditions, P53 is primarily negatively regulated by the MDM2 protein, a product of a proto-oncogene that inhibits apoptosis and promotes tumor cell proliferation [37, 38]. Our results showed that overexpression of HSP105 resulted in elevated levels of P53 and its downstream genes p21 and Bax, with inhibition of CDK4, Cyclin D1, Bcl-2 and MDM2 expression. In addition, the results of co-IP showed that there was an interaction between HSP105 and P53.

Among HSPs, HSP70, 90 and 105 are representatives of the proteins predominantly expressed after stress. HSP105, a member of the HSP70 superfamily, has functional and structural similarities in different in vitro and in vivo systems. However, the protein levels of HSP70 and HSP90 were also found in our study to be unchanged after the elevation or knockdown of HSP105, suggesting that these proteins have their own roles and that when one of them is impaired, the others have fewer compensatory effects (**Figure 5F**).

We provide evidence that upregulated expression of HSP105 suppresses the proliferation, migration and invasion of A431 and SCL-1 cell lines, promotes apoptosis and induces cell cycle arrest by activating the P53 signaling pathway. Silencing HSP105 had the opposite effect. This finding implies that HSP105 may be an important factor in regulating the development of cSCC. Due to its prominent role as a chaperone, HSP105 could serve as a new target of chemotherapy for cancer. In addition, a novel role for HSP105 in immune regulation has been described. In this regard, HSP105 overexpression in colorectal cancer cells induces the formation of macrophages with an anti-inflammatory profile [39]. Previous studies have shown that HSP105 is an immunogenic chaperone and a promising candidate for cancer vaccines. In a mouse model of cervical cancer, HSP105 was shown to not only enhance the antitumor potency of the cytotoxic T lympho-

cyte epitope E7 but also to significantly inhibit tumor growth [40].

In conclusion, HSP105 may play multiple roles in cancer cells because its chaperone function involves stabilizing oncogenic proteins and proteins involved in cancer signaling pathways. Our results suggest that upregulation of HSP-105 expression can inhibit cSCC development and progression by activating the P53 signaling pathway. Thus, targeting this chaperone has the potential to be an intervention tool in the fight against cancer, although the exact mechanisms involved in cancer development need to be further investigated.

Disclosure of conflict of interest

None.

Address correspondence to: Sheng Fang, Department of Dermatology, The First Affiliated Hospital of Chongqing Medical University, No. 1 Youyi Road, Yuzhong District, Chongqing 400016, China. E-mail: fangshengderm@163.com

References

[1] Tokez S, Venables ZC, Hollestein LM, Qi H, Bramer EM, Rentroia-Pacheco B, van den Bos RR, Rous B, Leigh IM, Nijsten T, Mooyaart AL and Wakkee M. Risk factors for metastatic cutaneous squamous cell carcinoma: refinement and replication based on 2 nationwide nested case-control studies. J Am Acad Dermatol 2022; 87: 64-71.

[2] Sow P, Dey S, Dey R, Majumder A, Nandi S, Bera M and Samadder A. Poly lactide-co-glycolide encapsulated nano-curcumin promoting antagonistic interactions between HSP 90 and XRCC1 proteins to prevent cypermethrin-induced toxicity: an in silico predicted in vitro and in vivo approach. Colloids Surf B Biointerfaces 2022; 220: 112905.

[3] Chakafana G and Shonhai A. The role of non-canonical Hsp70s (Hsp110/Grp170) in cancer. Cells 2021; 10: 254.

[4] Vos MJ, Hageman J, Carra S and Kampinga HH. Structural and functional diversities between members of the human HSPB, HSPH, HSPA, and DNAJ chaperone families. Biochemistry 2008; 47: 7001-7011.

[5] Pavlova NN, Zhu J and Thompson CB. The hallmarks of cancer metabolism: still emerging. Cell Metab 2022; 34: 355-377.

[6] Spano D, Heck C, De Antonellis P, Christofori G and Zollo M. Molecular networks that regulate cancer metastasis. Semin Cancer Biol 2012; 22: 234-249.

[7] Kai M, Nakatsura T, Egami H, Senju S, Nishimura Y and Ogawa M. Heat shock protein 105 is overexpressed in a variety of human tumors. Oncol Rep 2003; 10: 1777-1782.

[8] Gotoh K, Nonoguchi K, Higashitsuji H, Kaneko Y, Sakurai T, Sumitomo Y, Itoh K, Subjeck JR and Fujita J. Apg-2 has a chaperone-like activity similar to Hsp110 and is overexpressed in hepatocellular carcinomas. FEBS Lett 2004; 560: 19-24.

[9] Chan AT. Turning up the heat on colorectal cancer. Nat Med 2011; 17: 1186-1188.

[10] Yu N, Kakunda M, Pham V, Lill JR, Du P, Wongchenko M, Yan Y, Firestein R and Huang X. HSP105 recruits protein phosphatase 2A to dephosphorylate β-catenin. Mol Cell Biol 2015; 35: 1390-1400.

[11] Kawai T, Enomoto Y, Morikawa T, Matsushita H, Kume H, Fukayama M, Yamaguchi H, Kakimi K and Homma Y. High expression of heat shock protein 105 predicts a favorable prognosis for patients with urinary bladder cancer treated with radical cystectomy. Mol Clin Oncol 2014; 2: 38-42.

[12] Zheng Y, Yang Y, Wang J and Liang Y. Aberrant expression and high-frequency mutations of SHARPIN in nonmelanoma skin cancer. Exp Ther Med 2019; 17: 2746-2756.

[13] Lang BJ, Guerrero-Giménez ME, Prince TL, Ackerman A, Bonorino C and Calderwood SK. Heat shock proteins are essential components in transformation and tumor progression: cancer cell intrinsic pathways and beyond. Int J Mol Sci 2019; 20: 4507.

[14] Jia M, Li FZ, Ye Q, Chen KJ and Fang S. Expression of heat shock protein 105 in cutaneous squamous cell carcinoma: correlation with clinicopathological characteristics. Clin Cosmet Investig Dermatol 2021; 14: 633-641.

[15] Zhou M, Dong J, Huang J, Ye W, Zheng Z, Huang K, Pan Y, Cen J, Liang Y, Shu G, Ye S, Lu X and Zhang J. Chitosan-Gelatin-EGCG nanoparticle-meditated LncRNA TMEM44-AS1 silencing to activate the P53 signaling pathway for the synergistic reversal of 5-FU resistance in gastric cancer. Adv Sci (Weinh) 2022; 9: e2105077.

[16] Aparna M, Rao L, Kunhikatta V and Radhakrishnan R. The role of MMP-2 and MMP-9 as prognostic markers in the early stages of tongue squamous cell carcinoma. J Oral Pathol Med 2015; 44: 345-352.

[17] Fuchs EJ and Matzinger P. Is cancer dangerous to the immune system? Semin Immunol 1996; 8: 271-280.

[18] Roh BH, Kim DH, Cho MK, Park YL and Whang KU. Expression of heat shock protein 70 in human skin cells as a photoprotective function after UV exposure. Ann Dermatol 2008; 20: 184-189.

[19] Zininga T and Shonhai A. Small molecule inhibitors targeting the heat shock protein sys-

tem of human obligate protozoan parasites. Int J Mol Sci 2019; 20: 5930.
[20] Kalos M. HSP110 improves the anti-tumor effects of the cytotoxic T lymphocyte epitope E749-57 in mice: HSP110 as a peptide specific chaperone or adjuvant? Cancer Biol Ther 2010; 9: 333-334.
[21] Teshima H, Watanabe H, Yasutake R, Ikeda Y, Yonezu Y, Okamoto N, Kakihana A, Yuki R, Nakayama Y and Saito Y. Functional differences between Hsp105/110 family proteins in cell proliferation, cell division, and drug sensitivity. J Cell Biochem 2021; 122: 1958-1967.
[22] Gozzi GJ, Gonzalez D, Boudesco C, Dias AMM, Gotthard G, Uyanik B, Dondaine L, Marcion G, Hermetet F, Denis C, Hardy L, Suzanne P, Douhard R, Jego G, Dubrez L, Demidov ON, Neiers F, Briand L, Sopková-de Oliveira Santos J, Voisin-Chiret AS and Garrido C. Selecting the first chemical molecule inhibitor of HSP110 for colorectal cancer therapy. Cell Death Differ 2020; 27: 117-129.
[23] Yamagishi N, Saito Y and Hatayama T. Mammalian 105 kDa heat shock family proteins suppress hydrogen peroxide-induced apoptosis through a p38 MAPK-dependent mitochondrial pathway in HeLa cells. FEBS J 2008; 275: 4558-4570.
[24] Vidal Magalhães W, Gouveia Nogueira MF and Kaneko TM. Heat shock proteins (HSP): dermatological implications and perspectives. Eur J Dermatol 2012; 22: 8-13.
[25] Hatayama T, Yamagishi N, Minobe E and Sakai K. Role of hsp105 in protection against stress-induced apoptosis in neuronal PC12 cells. Biochem Biophys Res Commun 2001; 288: 528-534.
[26] Yamagishi N, Saito Y, Ishihara K and Hatayama T. Enhancement of oxidative stress-induced apoptosis by Hsp105alpha in mouse embryonal F9 cells. Eur J Biochem 2002; 269: 4143-4151.
[27] Dorard C, de Thonel A, Collura A, Marisa L, Svrcek M, Lagrange A, Jego G, Wanherdrick K, Joly AL, Buhard O, Gobbo J, Penard-Lacronique V, Zouali H, Tubacher E, Kirzin S, Selves J, Milano G, Etienne-Grimaldi MC, Bengrine-Lefèvre L, Louvet C, Tournigand C, Lefèvre JH, Parc Y, Tiret E, Fléjou JF, Gaub MP, Garrido C and Duval A. Expression of a mutant HSP110 sensitizes colorectal cancer cells to chemotherapy and improves disease prognosis. Nat Med 2011; 17: 1283-1289.
[28] Van Tubergen EA, Banerjee R, Liu M, Vander Broek R, Light E, Kuo S, Feinberg SE, Willis AL, Wolf G, Carey T, Bradford C, Prince M, Worden FP, Kirkwood KL and D'Silva NJ. Inactivation or loss of TTP promotes invasion in head and neck cancer via transcript stabilization and secretion of MMP9, MMP2, and IL-6. Clin Cancer Res 2013; 19: 1169-1179.
[29] Piipponen M, Riihilä P, Knuutila JS, Kallajoki M, Kähäri VM and Nissinen L. Super enhancer-regulated LINC00094 (SERLOC) upregulates the expression of MMP-1 and MMP-13 and promotes invasion of cutaneous squamous cell carcinoma. Cancers (Basel) 2022; 14: 3980.
[30] Kim JY, Kim N, Zheng Z, Lee JE and Yenari MA. The 70 kDa heat shock protein protects against experimental traumatic brain injury. Neurobiol Dis 2013; 58: 289-295.
[31] Ala-aho R, Grénman R, Seth P and Kähäri VM. Adenoviral delivery of p53 gene suppresses expression of collagenase-3 (MMP-13) in squamous carcinoma cells. Oncogene 2002; 21: 1187-1195.
[32] Page A, Navarro M, Suarez-Cabrera C, Alameda JP, Casanova ML, Paramio JM, Bravo A and Ramirez A. Protective role of p53 in skin cancer: carcinogenesis studies in mice lacking epidermal p53. Oncotarget 2016; 7: 20902-20918.
[33] Vousden KH and Prives C. Blinded by the light: the growing complexity of p53. Cell 2009; 137: 413-431.
[34] Kumagai J, Fukuda J, Kodama H, Murata M, Kawamura K, Itoh H and Tanaka T. Germ cell-specific heat shock protein 105 binds to p53 in a temperature-sensitive manner in rat testis. Eur J Biochem 2000; 267: 3073-3078.
[35] Hosaka S, Nakatsura T, Tsukamoto H, Hatayama T, Baba H and Nishimura Y. Synthetic small interfering RNA targeting heat shock protein 105 induces apoptosis of various cancer cells both in vitro and in vivo. Cancer Sci 2006; 97: 623-632.
[36] Oren M. Decision making by p53: life, death and cancer. Cell Death Differ 2003; 10: 431-442.
[37] Daujat S, Neel H and Piette J. MDM2: life without p53. Trends Genet 2001; 17: 459-464.
[38] Deb SP. Function and dysfunction of the human oncoprotein MDM2. Front Biosci 2002; 7: d235-243.
[39] Wang XY and Subjeck JR. High molecular weight stress proteins: identification, cloning and utilisation in cancer immunotherapy. Int J Hyperthermia 2013; 29: 364-375.
[40] Ren F, Xu Y, Mao L, Ou R, Ding Z, Zhang X, Tang J, Li B, Jia Z, Tian Z, Ni B and Wu Y. Heat shock protein 110 improves the antitumor effects of the cytotoxic T lymphocyte epitope E7(49-57) in mice. Cancer Biol Ther 2010; 9: 134-141.